


RESEARCH

Open Access



Segmentation of medial temporal subregions reveals early right-sided involvement in semantic variant PPA

Martina Bocchetta¹ , Juan Eugenio Iglesias², Lucy L. Russell¹, Caroline V. Greaves¹, Charles R. Marshall¹, Marzia A. Scelsi², David M. Cash^{1,2}, Sebastien Ourselin³, Jason D. Warren¹ and Jonathan D. Rohrer^{1*}

Abstract

Background: Semantic variant of primary progressive aphasia (svPPA) is a subtype of frontotemporal dementia characterized by asymmetric temporal atrophy.

Methods: We investigated the pattern of medial temporal lobe atrophy in 24 svPPA patients compared to 72 controls using novel approaches to segment the hippocampal and amygdalar subregions on MRIs. Based on semantic knowledge scores, we split the svPPA group into 3 subgroups of early, middle and late disease stage.

Results: Early stage: all left amygdalar and hippocampal subregions (except the tail) were affected in svPPA (21–35% smaller than controls), together with the following amygdalar nuclei in the right hemisphere: lateral, accessory basal and superficial (15–23%). On the right, only the temporal pole was affected among the cortical regions. Middle stage: the left hippocampal tail became affected (28%), together with the other amygdalar nuclei (22–26%), and CA4 (15%) on the right, with orbitofrontal cortex and subcortical structures involvement on the left, and more posterior temporal lobe on the right. Late stage: the remaining right hippocampal regions (except the tail) (19–24%) became affected, with more posterior left cortical and right extra-temporal anterior cortical involvement.

Conclusions: With advanced subregions segmentation, it is possible to detect early involvement of the right medial temporal lobe in svPPA that is not detectable by measuring the amygdala or hippocampus as a whole.

Keywords: Semantic variant PPA, Magnetic resonance imaging, Medial temporal subregions

Introduction

Semantic variant of primary progressive aphasia (svPPA) is a subtype of frontotemporal dementia (FTD), characterized clinically by anomia and impaired single-word comprehension. It is associated with a characteristic pattern of asymmetrical antero-inferior temporal lobe atrophy [1–3]. Previous studies of svPPA have shown early left medial temporal lobe involvement, with both hippocampal and amygdalar atrophy [4–6]. However, these studies have investigated the whole hippocampus or amygdala and no previous studies have looked at the

subregions of the medial temporal lobe. In this study, we therefore aimed to investigate the pattern of atrophy of the subregions of the hippocampus and the amygdala in svPPA, focusing on the involvement at different stages in order to understand the areas involved early in the disease process.

Methods

We reviewed the UCL Dementia Research Centre FTD MRI database to identify patients with a diagnosis of svPPA [7] and a usable 3 T T1-weighted magnetic resonance (MR) scan. Twenty-four patients were identified, all with left-temporal predominant disease. Seventy-two cognitively normal subjects with a usable volumetric 3 T T1-weighted MRI were identified as controls. The study

* Correspondence: j.rohrer@ucl.ac.uk

¹Dementia Research Centre, Department of Neurodegenerative Disease, UCL Queen Square Institute of Neurology, University College London, 8-11 Queen Square, London WC1N 3BG, UK

Full list of author information is available at the end of the article



was approved by the local ethics committee, and written informed consent was obtained from all participants. The study was conducted in accordance with the Helsinki Declaration of 1975.

Based on their scores on a test of semantic knowledge (the British Picture Vocabulary Scale, BPVS, a word-picture matching task) [8], we split the svPPA patients into three equal subgroups ($n = 8$ per group) of early (BPVS > 110/150), middle (BPVS = 55–110/150) and late disease stage (BPVS < 55/150). Patients were negative for mutations in all FTD-related genes. Two patients received post-mortem confirmation of the underlying neuropathology, both TDP-43 type C.

All patients underwent a detailed neuropsychological examination including tests of fluid intelligence (WASI Matrices), single-word comprehension (WASI Vocabulary), naming (Graded Naming Test), reading (National Adult Reading Test), verbal memory (Recognition Memory Test for Words), visual memory (Recognition Memory Test for Faces), short-term memory (forwards digit span), working memory (backwards digit span), calculation (Graded Difficulty Calculation Test), visuoperceptual function (Visual Object and Space Perception battery Object Decision subtest) and executive function (inhibition—D-KEFS Color-Word Ink Naming Test; abstract reasoning—WASI Similarities). A percentile score based on standard norms was generated for each patient, with a mean percentile score created for the early, middle and late stage groups. Assessment of behavioural symptoms was performed using the revised version of the Cambridge Behavioural Inventory (CBI-R) [9]: six subscores were used (difficulties with self-care, abnormal sleep, hallucinations/delusions, disinhibition, abnormal eating behaviour, obsessive-compulsive behaviour, apathy and loss of empathy) with a percentage of the total possible subscore generated for every patient; for each stage, a mean percentage score was created. We report the cognitive and behavioural profiles at each stage for illustrative purposes (Fig. 1 and Additional file 1: Table S1).

T1-weighted MRIs were acquired using a 3-T scanner, either a Trio (Siemens, Erlangen, Germany, TR = 2200 ms, TI = 900 ms, TE = 2.9 ms, acquisition matrix = 256×256 , spatial resolution = 1.1 mm) or a Prisma (Siemens, Erlangen, Germany, TR = 2000 ms, TI = 850 ms, TE = 2.93 ms, acquisition matrix = 256×256 , spatial resolution = 1.1 mm). Individuals with moderate to severe vascular disease or space-occupying lesions were excluded.

Volumetric MRI scans were first bias field corrected and whole-brain parcellated using the geodesic information flow (GIF) algorithm [10], which is based on atlas propagation and label fusion. The hippocampal subfields and amygdalar subregions were subsequently segmented using a customized version of the module available in FreeSurfer 6.0 [11, 12], to adapt the output of GIF to the

FreeSurfer format. For the hippocampal subfields, we focused on seven areas: CA1, CA2/CA3, CA4, dentate gyrus, subiculum, presubiculum and the tail. We excluded from the analysis the hippocampus-amygdala transition area, the parasubiculum, the molecular layer of the hippocampus, the fimbria and the hippocampal fissure, as they were too small, or not reliably delineated on T1-weighted images. For the amygdalar subnuclei, we focused the analysis on five regions, by combining the smallest subnuclei, based on an anatomical subdivision [13]: lateral nucleus, basal and paralaminar nucleus, accessory basal nucleus, cortico-amygdaloid transition area and the superficial nuclei (central nucleus, cortical nucleus, medial nucleus, anterior amygdaloid area).

For comparison with the medial temporal subregions, we extracted volumes of the following cortical regions from GIF: temporal (medial, lateral, supratemporal, temporal pole), frontal (orbitofrontal, prefrontal), parietal, occipital, insular and cingulate (anterior and posterior). We also extracted volumes of subcortical structures for the pallidum, putamen, caudate, nucleus accumbens and thalamus.

Left and right volumes were corrected for total intracranial volume (TIV), computed with SPM12 v6470 (Statistical Parametric Mapping, Wellcome Trust Centre for Neuroimaging, London, UK) running under Matlab R2014b (Math Works, Natick, MA, USA) [14]. All segmentations were visually checked for quality.

Statistical analyses were performed on brain volumes (as a percentage of TIV) in STATA v14 (Stata-Corp, College Station, TX), between control and patients (early, middle and late stage groups), using a linear regression test adjusting for scanner type, TIV, gender and age. The results were corrected for multiple comparisons (Bonferroni correction): $p < 0.006$ for amygdalar subnuclei and subcortical structures, $p < 0.005$ for hippocampal subfields and $p < 0.0035$ for cortical regions.

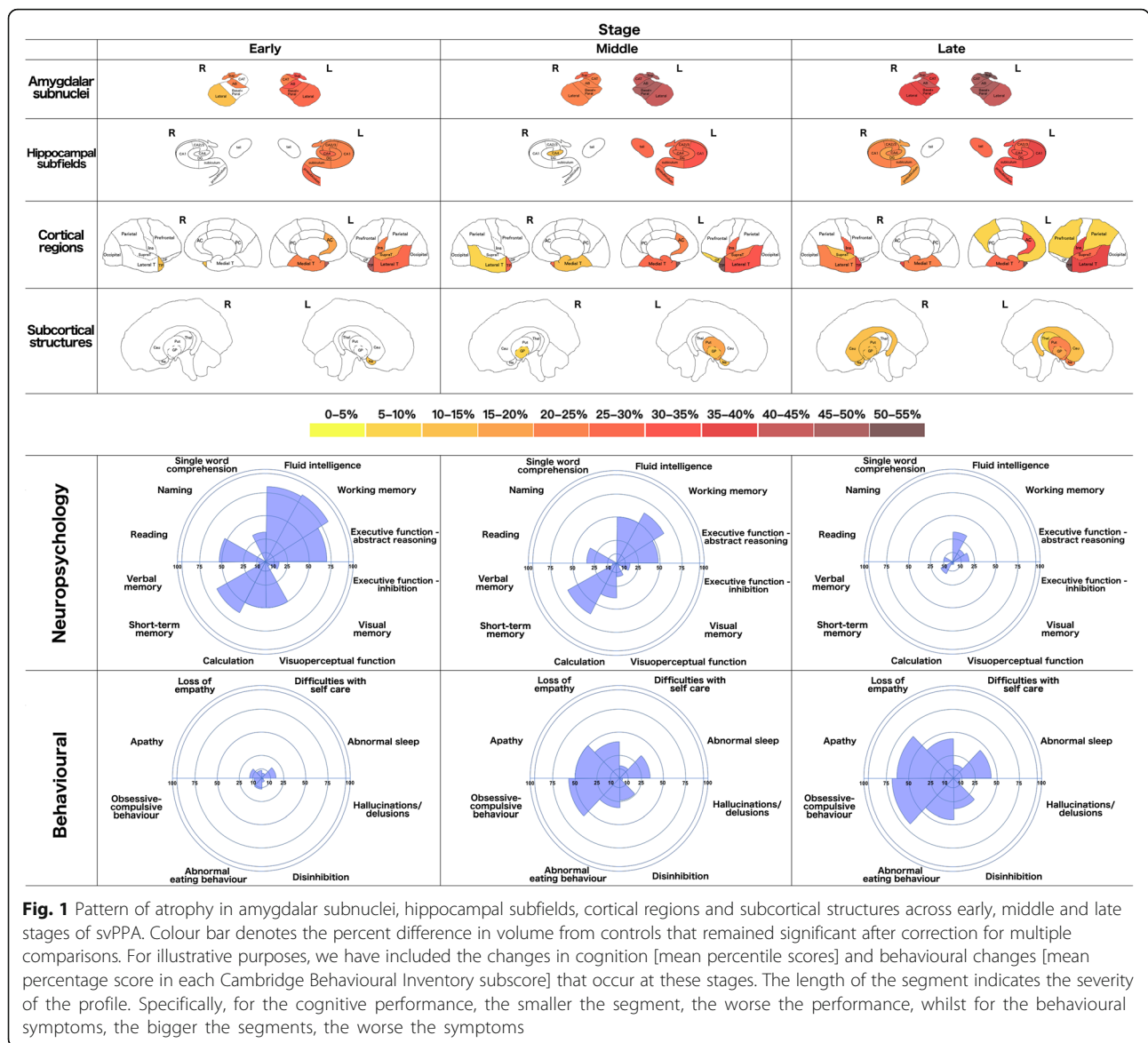
Results

No significant age difference was seen between any of the svPPA groups and controls [Early: 66.9 (5.5) years, Middle: 64.5 (9.5), Late: 64.2 (5.5); Controls: 61.0 (12.1)], $p = 0.112$, t test. However, there was a significant difference in gender distribution across stages [Early: 88% male, Middle: 63% male, Late: 25% male; Controls: 40% male], $p = 0.032$, Chi-square test.

Amygdalar subnuclei, hippocampal subfields, cortical regions, subcortical structures, neuropsychology performance and behavioural symptoms at each stage are shown in Fig. 1.

Early stage

All the left amygdalar and hippocampal subregions (except for the tail) were affected (24–35% and 21–27%



smaller than controls, $p < 0.0005$) at this stage, together with the right lateral, accessory basal and superficial nuclei of the amygdala (15–23%, $p < 0.004$) (Table 1).

Outside of the medial temporal lobe, on the left, all the temporal cortical regions (19–47%, $p < 0.0005$) were affected as well as the anterior cingulate (18%, $p = 0.001$) and insula (24%, $p < 0.0005$). The left nucleus accumbens was the only other subcortical structure affected (13%, $p < 0.0005$). Apart from the affected amygdalar subnuclei, the only other right hemisphere structure affected at this stage was the temporal pole (13%, $p = 0.006$).

Cognitively, patients showed severely impaired naming already, with relatively preserved working memory, abstract reasoning and fluid intelligence. Behavioural symptoms were mild and mainly related to abnormal eating behaviour, apathy and abnormal sleep.

Middle stage

At this stage, the left hippocampal tail became affected (28%, $p < 0.0005$), together with the other right amygdalar nuclei (22–26%, $p < 0.0005$) and the right CA4 region of the hippocampus (15%, $p = 0.003$).

Cortically, the left orbitofrontal lobe was affected at this stage along with more posterior temporal structures on the right: lateral and medial temporal cortices (9–12%, $p < 0.0005$). Subcortically, the left pallidum and putamen were affected (12–17%, $p < 0.0005$) and the right pallidum (8%).

Cognitively, single-word comprehension and reading became increasingly impaired, but working memory, short-term memory and abstract reasoning remained relatively intact. Behavioural symptoms increased with the presence of obsessive-compulsive behaviour and loss

Table 1 Volumetry of amygdalar subnuclei, hippocampal subfields, cortical regions and subcortical structures

	Controls				Early		Middle		Controls				Early		Middle	
	Left								Right							
	Mean	SD	%	p-value	%	p-value	%	p-value	Mean	SD	%	p-value	%	p-value	%	p-value
Amygdalar Subnuclei																
Lateral nucleus																
Controls	0.045	0.005							0.047	0.004						
Early	0.033	0.010	27	< 0.0005					0.040	0.006	15	0.003				
Middle	0.026	0.003	43	< 0.0005	23	< 0.0005			0.035	0.005	25	< 0.0005	12	0.005		
Late	0.025	0.003	44	< 0.0005	24	< 0.0005	2	0.723	0.030	0.005	36	< 0.0005	25	< 0.0005	14	0.017
Basal and paralaminar nucleus																
Controls	0.033	0.004							0.034	0.003						
Early	0.024	0.006	29	< 0.0005					0.029	0.006	15	0.012				
Middle	0.018	0.003	46	< 0.0005	24	< 0.0005			0.026	0.004	22	< 0.0005	8	0.092		
Late	0.017	0.002	48	< 0.0005	27	< 0.0005	4	0.483	0.021	0.003	39	< 0.0005	29	< 0.0005	22	< 0.0005
Accessory basal nucleus																
Controls	0.018	0.002							0.018	0.002						
Early	0.012	0.004	32	< 0.0005					0.015	0.004	21	< 0.0005				
Middle	0.010	0.002	46	< 0.0005	20	0.002			0.014	0.002	24	< 0.0005	4	0.373		
Late	0.009	0.001	49	< 0.0005	25	< 0.0005	6	0.482	0.011	0.002	42	< 0.0005	27	< 0.0005	24	0.002
Cortico-amygdaloid transition area																
Controls	0.012	0.002							0.012	0.001						
Early	0.009	0.002	24	< 0.0005					0.011	0.003	12	0.157				
Middle	0.007	0.001	44	< 0.0005	27	< 0.0005			0.009	0.002	24	< 0.0005	14	0.025		
Late	0.006	0.001	48	< 0.0005	32	< 0.0005	7	0.339	0.008	0.002	36	< 0.0005	28	< 0.0005	16	0.049
Superficial nuclei (Ce, Co, Me, AAA)																
Controls	0.011	0.002							0.012	0.002						
Early	0.007	0.002	35	< 0.0005					0.009	0.002	23	0.004				
Middle	0.006	0.001	47	< 0.0005	18	0.005			0.009	0.001	26	< 0.0005	4	0.341		
Late	0.005	0.001	51	< 0.0005	25	< 0.0005	9	0.275	0.007	0.002	41	< 0.0005	24	0.002	21	0.024
Hippocampal Subfields																
CA1																
Controls	0.044	0.005							0.047	0.006						
Early	0.035	0.005	22	< 0.0005					0.045	0.008	5	0.995				
Middle	0.031	0.007	31	< 0.0005	11	0.020			0.043	0.007	8	0.138	3	0.267		
Late	0.029	0.004	36	< 0.0005	18	0.001	7	0.268	0.036	0.006	24	< 0.0005	19	< 0.0005	17	0.003
CA2/CA3																
Controls	0.016	0.002							0.017	0.002						
Early	0.012	0.002	24	< 0.0005					0.016	0.004	6	0.931				
Middle	0.011	0.002	27	< 0.0005	3	0.460			0.015	0.003	12	0.064	7	0.184		
Late	0.012	0.002	26	< 0.0005	2	0.518	-1	0.945	0.013	0.002	24	< 0.0005	19	0.002	13	0.054
CA4																
Controls	0.018	0.002							0.019	0.002						
Early	0.013	0.002	27	< 0.0005					0.017	0.004	10	0.281				
Middle	0.013	0.001	27	< 0.0005	1	0.342			0.016	0.002	15	0.003	5	0.156		
Late	0.012	0.001	34	< 0.0005	9	0.007	9	0.066	0.015	0.002	21	< 0.0005	13	0.004	8	0.111

Table 1 Volumetry of amygdalar subnuclei, hippocampal subfields, cortical regions and subcortical structures (Continued)

	Controls				Early		Middle		Controls				Early		Middle	
	Left								Right							
	Mean	SD	%	p-value	%	p-value	%	p-value	Mean	SD	%	p-value	%	p-value	%	p-value
Dentate gyrus																
Controls	0.021	0.002							0.021	0.002						
Early	0.016	0.002	25	< 0.0005					0.020	0.005	7	0.759				
Middle	0.015	0.002	27	< 0.0005	4	0.183			0.019	0.003	13	0.021	6	0.132		
Late	0.014	0.002	32	< 0.0005	10	0.011	6	0.185	0.017	0.003	19	< 0.0005	14	0.003	8	0.117
Subiculum																
Controls	0.028	0.003							0.029	0.003						
Early	0.022	0.002	21	< 0.0005					0.028	0.006	1	0.425				
Middle	0.020	0.003	28	< 0.0005	10	0.048			0.026	0.005	8	0.116	8	0.074		
Late	0.020	0.004	31	< 0.0005	13	0.005	4	0.338	0.022	0.005	23	< 0.0005	23	< 0.0005	16	0.004
Presubiculum																
Controls	0.023	0.003							0.022	0.003						
Early	0.017	0.002	27	< 0.0005					0.023	0.006	-2	0.173				
Middle	0.016	0.002	30	< 0.0005	5	0.362			0.021	0.007	5	0.942	6	0.267		
Late	0.016	0.003	33	< 0.0005	8	0.045	3	0.245	0.018	0.005	19	0.001	20	0.001	15	0.015
Hippocampal tail																
Controls	0.041	0.005							0.041	0.005						
Early	0.034	0.006	18	0.019					0.043	0.010	-4	0.055				
Middle	0.030	0.005	28	< 0.0005	12	0.026			0.042	0.010	-2	0.371	2	0.41		
Late	0.029	0.006	29	< 0.0005	13	0.009	2	0.624	0.037	0.008	8	0.084	12	0.008	10	0.054
Cortical Regions																
Orbitofrontal																
Controls	0.697	0.047							0.716	0.048						
Early	0.682	0.045	2	0.934					0.727	0.057	-2	0.158				
Middle	0.629	0.089	10	0.001	8	0.015			0.716	0.046	0	0.806	1	0.362		
Late	0.637	0.063	9	0.009	7	0.062	-1	0.612	0.697	0.078	3	0.647	4	0.166	3	0.604
Prefrontal cortex																
Controls	4.216	0.230							4.322	0.224						
Early	4.087	0.337	3	0.691					4.299	0.379	1	0.545				
Middle	4.045	0.529	4	0.112	1	0.373			4.380	0.369	-1	0.506	-2	0.977		
Late	3.806	0.250	10	0.002	7	0.047	6	0.245	4.119	0.269	5	0.201	4	0.168	6	0.153
Anterior cingulate																
Controls	0.382	0.039							0.283	0.042						
Early	0.315	0.041	18	0.001					0.289	0.046	-2	0.339				
Middle	0.300	0.068	22	< 0.0005	5	0.311			0.318	0.069	-13	0.008	-10	0.204		
Late	0.255	0.026	33	< 0.0005	19	0.002	15	0.023	0.288	0.058	-2	0.968	0	0.457	9	0.047
Posterior cingulate																
Controls	0.359	0.038							0.343	0.035						
Early	0.350	0.020	3	0.609					0.368	0.019	-7	0.009				
Middle	0.332	0.025	7	0.065	5	0.320			0.365	0.028	-6	0.022	1	0.747		
Late	0.337	0.028	6	0.169	4	0.535	-1	0.728	0.361	0.047	-5	0.150	2	0.348	1	0.523

Table 1 Volumetry of amygdalar subnuclei, hippocampal subfields, cortical regions and subcortical structures (Continued)

	Controls				Early		Middle		Controls				Early		Middle	
	Left								Right							
	Mean	SD	%	p-value	%	p-value	%	p-value	Mean	SD	%	p-value	%	p-value	%	p-value
Parietal																
Controls	3.224	0.211							3.186	0.229						
Early	3.143	0.229	3	0.538					3.216	0.248	-1	0.049				
Middle	3.147	0.249	2	0.709	0	0.450			3.272	0.200	-3	0.053	-2	0.944		
Late	2.993	0.234	7	0.003	5	0.008	5	0.046	3.142	0.213	1	0.793	2	0.096	4	0.105
Occipital																
Controls	2.473	0.207							2.564	0.205						
Early	2.393	0.227	3	0.835					2.538	0.195	1	0.575				
Middle	2.395	0.155	3	0.552	0	0.776			2.552	0.175	0	0.697	-1	0.887		
Late	2.432	0.148	2	0.733	-2	0.926	-2	0.853	2.572	0.147	0	0.796	-1	0.817	-1	0.924
Insula																
Controls	0.370	0.035							0.381	0.039						
Early	0.281	0.032	24	< 0.0005					0.343	0.049	10	0.110				
Middle	0.260	0.036	30	< 0.0005	7	0.064			0.337	0.038	12	0.007	2	0.425		
Late	0.229	0.021	38	< 0.0005	18	< 0.0005	12	0.013	0.267	0.039	30	< 0.0005	22	< 0.0005	21	< 0.0005
Medial temporal																
Controls	1.012	0.062							1.041	0.067						
Early	0.785	0.057	22	< 0.0005					0.981	0.070	6	0.076				
Middle	0.730	0.056	28	< 0.0005	7	0.042			0.915	0.070	12	< 0.0005	7	0.044		
Late	0.743	0.058	27	< 0.0005	5	0.088	-2	0.787	0.791	0.074	24	< 0.0005	19	< 0.0005	14	< 0.0005
Lateral temporal																
Controls	2.304	0.153							2.345	0.143						
Early	1.652	0.201	28	< 0.0005					2.231	0.134	5	0.133				
Middle	1.554	0.150	33	< 0.0005	6	0.084			2.137	0.099	9	< 0.0005	4	0.105		
Late	1.384	0.159	40	< 0.0005	16	< 0.0005	11	0.026	1.864	0.217	21	< 0.0005	16	< 0.0005	13	< 0.0005
Temporal pole																
Controls	0.488	0.056							0.477	0.055						
Early	0.261	0.066	47	< 0.0005					0.413	0.071	13	0.006				
Middle	0.231	0.035	53	< 0.0005	12	0.187			0.352	0.049	26	< 0.0005	15	0.019		
Late	0.228	0.029	53	< 0.0005	13	0.324	1	0.766	0.287	0.038	40	< 0.0005	30	< 0.0005	18	0.048
Supratemporal																
Controls	0.430	0.050							0.369	0.039						
Early	0.348	0.037	19	< 0.0005					0.357	0.045	3	0.910				
Middle	0.336	0.046	22	< 0.0005	4	0.359			0.368	0.040	0	0.718	-3	0.855		
Late	0.301	0.056	30	< 0.0005	14	0.017	10	0.122	0.322	0.054	13	0.004	10	0.028	12	0.016
Subcortical Structures																
Nucleus accumbens																
Controls	0.040	0.003							0.038	0.003						
Early	0.035	0.003	13	< 0.0005					0.035	0.003	9	0.048				
Middle	0.034	0.005	15	< 0.0005	3	0.235			0.036	0.004	5	0.155	-4	0.638		
Late	0.030	0.003	24	< 0.0005	13	0.001	10	0.019	0.032	0.004	15	< 0.0005	7	0.026	11	0.007

Table 1 Volumetry of amygdalar subnuclei, hippocampal subfields, cortical regions and subcortical structures (Continued)

	Controls				Early		Middle		Controls				Early		Middle	
	Left								Right							
	Mean	SD	%	p-value	%	p-value	%	p-value	Mean	SD	%	p-value	%	p-value	%	p-value
Caudate																
Controls	0.237	0.026							0.248	0.024						
Early	0.221	0.020	7	0.508					0.235	0.026	5	0.598				
Middle	0.222	0.026	6	0.350	0	0.851			0.237	0.024	4	0.507	-1	0.929		
Late	0.207	0.030	12	0.001	6	0.037	7	0.053	0.217	0.036	12	0.001	8	0.044	8	0.050
Pallidum																
Controls	0.129	0.014							0.130	0.013						
Early	0.114	0.007	12	0.010					0.119	0.007	8	0.123				
Middle	0.113	0.008	12	<0.0005	1	0.160			0.119	0.008	8	0.004	0	0.303		
Late	0.104	0.009	19	<0.0005	9	0.016	8	0.270	0.111	0.011	14	<0.0005	6	0.054	7	0.336
Putamen																
Controls	0.307	0.031							0.305	0.031						
Early	0.268	0.018	13	0.011					0.289	0.016	5	0.981				
Middle	0.255	0.023	17	<0.0005	5	0.044			0.277	0.023	9	0.019	4	0.081		
Late	0.237	0.018	23	<0.0005	11	0.001	7	0.144	0.261	0.022	14	<0.0005	10	0.002	6	0.142
Thalamus																
Controls	0.400	0.035							0.392	0.039						
Early	0.357	0.024	11	0.024					0.380	0.032	3	0.279				
Middle	0.362	0.029	9	0.008	-2	0.791			0.387	0.036	1	0.258	-2	0.992		
Late	0.364	0.027	9	<0.0005	-2	0.169	-1	0.255	0.388	0.027	1	0.226	-2	0.093	0	0.086

Values denote mean and standard deviation (SD) volumes as the percentage of the total intracranial volume (TIV) or difference (%). p values denote significance on linear regression test. Bold represents a significant difference between the groups after correcting for multiple comparisons

of empathy as well as abnormal eating behaviour, apathy and disinhibition.

Late stage

In the late stage, the remaining right hippocampal regions (except the tail) (19–24%, $p < 0.001$) became affected.

Cortically, spread to the left prefrontal and parietal cortices was seen whilst on the right, the insula (30%) and supratemporal cortex (13%, $p < 0.004$) were affected. Subcortically, the left caudate, thalamus and right nucleus accumbens, caudate and putamen were affected (12–15%).

At this stage, all cognitive domains were severely impaired except for short-term and working memory, abstract reasoning and fluid intelligence. Severe behavioural symptoms were seen.

Discussion

Using advanced subregional segmentation, we were able to detect early involvement in the right hemisphere in svPPA, with progression of atrophy through the medial temporal lobes as the disease moves from early to middle to late stage.

Extensive medial temporal atrophy is seen on the left in most amygdalar and hippocampal subregions at the earliest stage of svPPA, co-incidental with the involvement of all of the temporal cortices on the left. This is consistent with previous studies showing that even at first clinical presentation, significant left temporal lobe atrophy is present [1, 15].

Previous studies have not shown early involvement of the right medial temporal structures. In this study, the earliest subnuclei affected on the right were the accessory basal, lateral and superficial nuclei of the amygdala. These subnuclei are interconnected and receive input from the temporal pole and the hippocampus (also affected on the right in the early stage) as well as other parts of the temporal and frontal cortices and the nucleus accumbens [13, 16]. The ability to use advanced subregional segmentation techniques in this study allows early detection of right medial temporal atrophy.

The cognitive and behavioural correlates of the individual right amygdalar subnuclei are poorly studied, but prior studies of the whole amygdala implicate the right side as being important in the processing of emotional information [17, 18]. In our

study, loss of empathy is mildly affected at the earliest stage (Fig. 1); this is likely to represent an impairment of self-knowledge, a process that requires the linking of emotions with semantics, and has previously been shown to be associated with right temporal lobe atrophy including the amygdala [19]. The particular amygdalar subnuclei affected early are part of the limbic network and therefore likely to be intrinsically involved in emotion processing [16].

Of all the medial temporal subregions, the hippocampal tail is preserved until the later stages of svPPA. This is in line with previous studies, where the posterior temporal lobe is spared and an antero-posterior gradient is present [20, 21]. Indeed, svPPA patients typically show intact episodic memory and spatial navigation, functions typically linked to the hippocampal tail. Consistent with the theory of svPPA as a network-opathy [22], the first hippocampal region to become affected on the right is CA4, an area highly connected to the temporal cortex and amygdala [23].

Limitations of the study include using cross-sectional data with staging of the disease by impairment on a task of semantic knowledge and the small number of svPPA cases. Further studies would benefit from the analysis of longitudinal data from a larger sample to see whether the same pattern is seen. Despite the gold standard still being manual segmentation of dedicated MRIs or on brain tissue post-mortem, these automated methods included in this study have been previously validated and proven reliable to delineate the subregions on T1-MRI (Dice coefficients > 0.86; ICC 0.88–0.93) [10–12, 24, 25]. Moreover, in this study, we carefully excluded small subregions and combined together groups of nuclei to improve the anatomical validity. Automated segmentations will play a key role in the future, as manual segmentations are likely to be unfeasible for large cohorts of patients.

Additional file

Additional file 1: Table S1. Cognitive and behavioural variables for the svPPA patients. *p* values denote significance on Kruskal-Wallis test among the three groups. (DOCX 17 kb)

Acknowledgements

Not applicable.

Funding

The Dementia Research Centre is supported by Alzheimer's Research UK, Brain Research Trust and The Wolfson Foundation. This work was supported by the NIHR Queen Square Dementia Biomedical Research Unit and the NIHR UCL/H Biomedical Research Centre, the MRC UK GENFI grant (MR/M023664/1) and the Alzheimer's Society (AS-PG-16-007). JDR is supported by an MRC Clinician Scientist Fellowship (MR/M008525/1) and has received funding from the NIHR Rare Disease Translational Research Collaboration (BRC149/NS/MH). JDW was supported by a Wellcome Trust Senior Clinical Fellowship (091673/Z/10/Z), and his research is supported by the Alzheimer's

Society, Alzheimer's Research UK and the NIHR UCLH Biomedical Research Centre. SO is funded by the Engineering and Physical Sciences Research Council (EP/H046410/1, EP/J020990/1, EP/K005278), the Medical Research Council (MR/J01107X/1), the EU-FP7 project VPH-DARE@IT (FP7- ICT-2011-9-601055) and the National Institute for Health Research University College London Hospitals Biomedical Research Centre (NIHR BRC UCLH/UCL High Impact Initiative BW.mn.BRC10269). JEI is supported by the European Research Council (Starting Grant 677697, project BUNGEE-TOOLS). MAS acknowledges the financial support by the EPSRC-funded UCL Centre for Doctoral Training in Medical Imaging (EP/L016478/1).

Availability of data and materials

The datasets used and analysed during the current study are available from the corresponding author on reasonable request.

Authors' contributions

MB drafted the body of the manuscript, tables and figures and ran the analyses. JDR contributed to the design and concept of the study. JEI contributed to the data analyses. LLR, CVG, CRM, JDW and JDR were responsible for the collection of data and recruitment of patients. All authors critically reviewed and approved the final manuscript and contributed to the data interpretation.

Ethics approval and consent to participate

This study was approved by the London Queen Square NRES Committee. Written informed consent was obtained from all participants.

Consent for publication

Not applicable.

Competing interests

JDR has been on a Medical Advisory Board for Wave Life Sciences and Ionis Pharmaceuticals. All other authors declare that they have no competing interests.

Publisher's Note

Springer Nature remains neutral with regard to jurisdictional claims in published maps and institutional affiliations.

Author details

¹Dementia Research Centre, Department of Neurodegenerative Disease, UCL Queen Square Institute of Neurology, University College London, 8-11 Queen Square, London WC1N 3BG, UK. ²Centre for Medical Image Computing, Department of Medical Physics and Biomedical Engineering, University College London, London, UK. ³School of Biomedical Engineering and Imaging Sciences, St Thomas' Hospital, King's College London, London, UK.

Received: 3 January 2019 Accepted: 2 April 2019

Published online: 10 May 2019

References

- Rohrer JD, Warren JD, Modat M, Ridgway GR, Douiri A, Rossor MN, Ourselin S, Fox NC. Patterns of cortical thinning in the language variants of frontotemporal lobar degeneration. *Neurology*. 2009;72(18):1562–9.
- Rohrer JD, Rosen HJ. Neuroimaging in frontotemporal dementia. *Int Rev Psychiatry*. 2013;25(2):221–9.
- Schroeter ML, Raczka K, Neumann J, Yves von Cramon D. Towards a nosology for frontotemporal lobar degenerations—a meta-analysis involving 267 subjects. *Neuroimage*. 2007;36(3):497–510.
- Rohrer JD, McNaught E, Foster J, Clegg SL, Barnes J, Omar R, Warrington EK, Rossor MN, Warren JD, Fox NC. Tracking progression in frontotemporal lobar degeneration: serial MRI in semantic dementia. *Neurology*. 2008; 71(18):1445–51.
- Lehmann M, Douiri A, Kim LG, Modat M, Chan D, Ourselin S, Barnes J, Fox NC. Atrophy patterns in Alzheimer's disease and semantic dementia: a comparison of FreeSurfer and manual volumetric measurements. *Neuroimage*. 2010;49(3):2264–74.
- Nestor PJ, Fryer TD, Hodges JR. Declarative memory impairments in Alzheimer's disease and semantic dementia. *Neuroimage*. 2006;30(3): 1010–20.

7. Gorno-Tempini ML, Hillis AE, Weintraub S, Kertesz A, Mendez M, Cappa SF, Ogar JM, Rohrer JD, Black S, Boeve BF, Manes F, Dronkers NF, Vandenberghe R, Rascovsky K, Patterson K, Miller BL, Knopman DS, Hodges JR, Mesulam MM, Grossman M. Classification of primary progressive aphasia and its variants. *Neurology*. 2011;76(11):1006–14.
8. Dunn DM, Dunn LM, National Foundation for Educational Research in England and Wales, GL Assessment (Firm). 2009. 3rd ed. *GL Assessment*. ISBN-10: 0708719554.
9. Wear HJ, Wedderburn CJ, Mioshi E, Williams-Gray CH, Mason SL, Barker RA, Hodges JR. The Cambridge Behavioural Inventory revised. *Dement Neuropsychol*. 2008;2(2):102–7.
10. Cardoso MJ, Modat M, Wolz R, Melbourne A, Cash D, Rueckert D, Ourselin S. Geodesic information flows: spatially-variant graphs and their application to segmentation and fusion. *IEEE TMI*. 2015. <https://doi.org/10.1109/TMI.2015.2418298>.
11. Saygin ZM, Kliemann D, Iglesias JE, van der Kouwe AJW, Boyd E, Reuter M, Stevens A, Van Leemput K, McKee A, Frosch MP, Fischl B, Augustinack JC, Alzheimer's Disease Neuroimaging Initiative. High-resolution magnetic resonance imaging reveals nuclei of the human amygdala: manual segmentation to automatic atlas. *Neuroimage*. 2017;155:370–82.
12. Iglesias JE, Augustinack JC, Nguyen K, Player CM, Player A, Wright M, Roy N, Frosch MP, McKee AC, Wald LL, Fischl B, Van Leemput K. A computational atlas of the hippocampal formation using ex vivo, ultra-high resolution MRI: application to adaptive segmentation of in vivo MRI. *Neuroimage*. 2015;115:117–37.
13. deCampo DM, Fudge JL. Where and what is the paralaminar nucleus? A review on a unique and frequently overlooked area of the primate amygdala. *Neurosci Biobehav Rev*. 2012;36(1):520–35.
14. Malone IB, Leung KK, Clegg S, Barnes J, Whitwell JL, Ashburner J, Fox NC, Ridgway GR. Accurate automatic estimation of total intracranial volume: a nuisance variable with less nuisance. *Neuroimage*. 2015;104:366–72.
15. Czarnecki K, Duffy JR, Nehl CR, Cross SA, Molano JR, Jack CR Jr, Shiung MM, Josephs KA, Boeve BF. Very early semantic dementia with progressive temporal lobe atrophy: an 8-year longitudinal study. *Arch Neurol*. 2008;65(12):1659–63.
16. LeDoux J. The amygdala. *Curr Biol*. 2007;17(20):R868–74.
17. Rosen HJ, Perry RJ, Murphy J, Kramer JH, Mychack P, Schuff N, Weiner M, Levenson RW, Miller BL. Emotion comprehension in the temporal variant of frontotemporal dementia. *Brain*. 2002;125(Pt 10):2286–95.
18. Snowden JS, Harris JM, Thompson JC, Koblecki C, Jones M, Richardson AM, Neary D. Semantic dementia and the left and right temporal lobes. *Cortex*. 2017. <https://doi.org/10.1016/j.cortex.2017.08.024>.
19. Sollberger M, Rosen HJ, Shany-Ur T, Ullah J, Stanley CM, Laluz V, Weiner MW, Wilson SM, Miller BL, Rankin KP. Neural substrates of socioemotional self-awareness in neurodegenerative disease. *Brain Behav*. 2014;4(2):201–14.
20. La Joie R, Perrotin A, de La Sayette V, Egret S, Doeuvre L, Belliard S, Eustache F, Desgranges B, Chételat G. Hippocampal subfield volumetry in mild cognitive impairment, Alzheimer's disease and semantic dementia. *Neuroimage Clin*. 2013;3:155–62.
21. Tan RH, Wong S, Kril JJ, Piguet O, Hornberger M, Hodges JR, Halliday GM. Beyond the temporal pole: limbic memory circuit in the semantic variant of primary progressive aphasia. *Brain*. 2014;137(Pt 7):2065–76.
22. Fletcher PD, Warren JD. Semantic dementia: a specific network-opathy. *J Mol Neurosci*. 2011;45(3):629–36.
23. de Flores R, Mutlu J, Bejanin A, Gonneaud J, Landeau B, Tomadesso C, Mézange F, de La Sayette V, Eustache F, Chételat G. Intrinsic connectivity of hippocampal subfields in normal elderly and mild cognitive impairment patients. *Hum Brain Mapp*. 2017;38(10):4922–32.
24. Herten A, Konrad K, Krinzing H, Seitz J, von Polier GG. Accuracy and bias of automatic hippocampal segmentation in children and adolescents. *Brain Struct Funct*. 2018. <https://doi.org/10.1007/s00429-018-1802-2>.
25. Whelan CD, Hibar DP, van Velzen LS, Zannas AS, Carrillo-Roa T, McMahon K, Prasad G, Kelly S, Faskowitz J, deZubiracay G, Iglesias JE, van Erp TGM, Frodl T, Martin NG, Wright MJ, Jahanshad N, Schmaal L, Sämann PG, Thompson PM, Alzheimer's Disease Neuroimaging Initiative. Heritability and reliability of automatically segmented human hippocampal formation subregions. *Neuroimage*. 2016;128:125–37.

Ready to submit your research? Choose BMC and benefit from:

- fast, convenient online submission
- thorough peer review by experienced researchers in your field
- rapid publication on acceptance
- support for research data, including large and complex data types
- gold Open Access which fosters wider collaboration and increased citations
- maximum visibility for your research: over 100M website views per year

At BMC, research is always in progress.

Learn more biomedcentral.com/submissions

